ARTICLE
Journal of Cellular Biochemistry 115:1955–1966 (2014)

Journal of Cellular Biochemistry

Paracrine Stimulation of P2X7 Receptor by ATP Activates a Proliferative Pathway in Ovarian Carcinoma Cells

Francisco G. Vázquez-Cuevas,[1]* Angélica S. Martínez-Ramírez,[1] Leticia Robles-Martínez,[1] Edith Garay,[1] Alejandro García-Carrancá,[2,3] Delia Pérez-Montiel,[4] Carolina Castañeda-García,[1] and Rogelio O. Arellano[1]

[1]*Departamento de Neurobiología Celular y Molecular, Instituto de Neurobiología, Universidad Nacional Autónoma de México, Boulevard Juriquilla 3001, Juriquilla Querétaro CP 76230, México*

[2]*Laboratorio de Virus y Cáncer Unidad de Investigación Biomédica en Cáncer, Instituto de Investigaciones Biomédicas-Universidad Nacional Autónoma de México, Av. San Fernando #22, Colonia Sección XVI, Tlalpan CP 14080, DF, México*

[3]*División de Investigación Básica, Instituto Nacional de Cancerología, Secretaría de Salud, México, Av. San Fernando #22, Colonia Sección XVI, Tlalpan CP 14080, DF, México*

[4]*Departamento de Patología, Instituto Nacional de Cancerología, Secretaría de Salud, México Av. San Fernando #22, Colonia Sección XVI, Tlalpan CP 14080, DF, México*

ABSTRACT

P2X7 is a purinergic receptor-channel; its activation by ATP elicits a broad set of cellular actions, from apoptosis to signals for survival. Here, P2X7 expression and function was studied in human ovarian carcinoma (OCA) cells, and biopsies from non-cancerous and cancer patients were analyzed by immunohistochemistry. Ovarian surface epithelium in healthy tissue expressed P2X7 at a high level that was maintained throughout the cancer. The cell lines SKOV-3 and CAOV-3 were used to investigate P2X7 functions in OCA. In SKOV-3 cells, selective stimulation of P2X7 by 2′(3′)-O-(4-benzoylbenzoyl) adenosine-5′-triphosphate (BzATP) induced a dose-dependent increase of intracellular Ca^{2+} concentration ($[Ca^{2+}]_i$) but not cell death. Instead, BzATP increased the levels of phosphorylated ERK and AKT (pERK and pAKT), with an EC_{50} of 44 ± 2 and 1.27 ± 0.5 μM, respectively; 10 μM BzATP evoked a maximum effect within 15 min that lasted for 120 min. Interestingly, basal levels of pERK and pAKT were decreased in the presence of apyrase in the medium, strongly suggesting an endogenous, ATP-mediated phenomenon. Accordingly: (i) mechanically stimulated cells generated a $[Ca^{2+}]_i$ increase that was abolished by apyrase; (ii) apyrase induced a decrease in culture viability, as measured by the MTS assay for mitochondrial activity; and (iii) incubation with 10 μM AZ10606120, a specific P2X7 antagonist and transfection with the dominant negative P2X7 mutant E496A, both reduced cell viability to $70.1 \pm 8.9\%$ and to $76.5 \pm 5\%$, respectively, of control cultures. These observations suggested that P2X7 activity was auto-induced through ATP efflux; this increased pERK and pAKT levels that generated a positive feedback on cell viability. J. Cell. Biochem. 115: 1955–1966, 2014.

KEY WORDS: P2X7 RECEPTOR; OVARIAN SURFACE EPITHELIUM; OVARIAN CANCER

Ovarian carcinoma (OCA) is the most common gynecologic disease in Western and Northern Europe and the United States [Runnebaum and Stickeler, 2001]. Evidence supports the hypothesis that 90% of ovarian cancers originate in the ovarian surface epithelium (OSE) [Auersperg et al., 2001; Murdoch and McDonnel, 2002]; cancers derived from this epithelium contain highly invasive metastatic cells that rapidly spread to other organs such as the uterus, lung, liver [Munkarah et al., 1997]; and brain [Cormio et al., 1995]. Recent studies on the tumor microenvironment have attempted to identify the role of local modulators such as ATP, which has been associated with cancer cell growth regulation [Hanahan and Weinberg, 2011].

The purinergic system regulates a broad range of cell functions [Burnstock, 2007] in somatic ovarian cells several studies have

Grant sponsor: Consejo Nacional de Ciencia y Tecnología, México; Grant number: 166725; Grant sponsor: Programa de Apoyo a Proyectos de Investigación e Innovación Tecnológica UNAM, México; Grant numbers: IN205114, IA200112, IN205312.

*Correspondence to: Dr. Francisco Gabriel Vázquez-Cuevas, Instituto de Neurobiología, Universidad Nacional Autónoma de México, Boulevard Juriquilla 3001, Juriquilla Querétaro, CP 76230, Mexico. E-mail: fvazquezc132005@yahoo.com.mx

Manuscript Received: 22 April 2014; Manuscript Accepted: 2 June 2014

Accepted manuscript online in Wiley Online Library (wileyonlinelibrary.com): 10 June 2014

DOI 10.1002/jcb.24867 • © 2014 Wiley Periodicals, Inc.

suggested that ATP, acting as a local signal, is a modulator [Tai et al., 2001; Arellano et al., 2002; Vázquez-Cuevas et al., 2006; Arellano et al., 2009; Vázquez-Cuevas et al., 2013] of normal functions of the ovary, such as the steroidogenic response to luteinizing hormone [Tai et al., 2001] or a potential mediator of cell death in the ovulatory process [Vázquez-Cuevas et al., 2013]. However, its possible role in diverse ovarian pathologies and particularly OCA has not been investigated.

ATP exerts its action as an intercellular signal through specific receptors named P2; two subfamilies are known: P2Y, which are G-protein coupled receptors, and P2X, which are receptor-channels operated by ligand. Seven genes coding for subunits P2X1 to P2X7 have been cloned. The P2X receptor-channel is trimeric and mainly permeable to Ca^{2+}, Na^{+}, and K^{+} ions [Coddou et al., 2011]. The P2X7 subunit forms homotrimeric channels that generate a non-desensitizing current response, and in a variety of cell types their activation induces apoptotic cell death through cytoplasmic Ca^{2+} overload [Di Virgilio et al., 1998; Coutinho-Silva et al., 1999; Coddou et al., 2011]. Nevertheless, it is also well documented that stimulation of P2X7 is able to activate ERK [Panenka et al., 2001; Bradford and Soltoff, 2002; Stefano et al., 2007] and AKT [Jacques-Silva et al., 2004; Ortega et al., 2009; Tafani et al., 2011] proteins that are important in cell cycle regulation. It has also been demonstrated that P2X7 activation promotes cell proliferation in some cases [Baricordi et al., 1996; Thompson et al., 2012; Zou et al., 2012].

Given that P2X7 receptors participate in both apoptosis and cell proliferation, they have been investigated in relation to the phenomenon of oncogenic transformation in a variety of tissues. For example, in human endometrial epithelium the expression of P2X7 is down-regulated [Li et al., 2007]; a reduction in its expression has also been reported in epithelial cancer cells from the ectodermal, urogenital, and distal paramesonephric sinus [Li et al., 2009]. In contrast, P2X7, which is not detectable in healthy prostate tissue, becomes strongly expressed in adenocarcinoma; this has been proposed as a marker of malignant transformation [Slater et al., 2004a]. Similar findings have been reported for human thyroid papillary carcinoma [Solini et al., 2007] and mammary gland [Slater et al., 2004b].

Recent evidence strongly suggests that the purinergic system has an important role in tumor growth [Di Virgilio et al., 2009; Adinolfi et al., 2012], through a regulatory loop that favors proliferation and has at least three elements: (1) An increased metabolic level in tumor cells [Nakajima and Van Houten, 2012]; (2) increased ATP efflux towards the tumor interstitium [Pellegatti et al., 2008]; and (3) increased expression of purinergic receptors [Slater et al., 2004a,b; Solini et al., 2007]. Finally, the evidence presented also supports the notion that in some cell types, P2X7 activation might be an important element of this proliferative loop [Adinolfi et al., 2012].

Here, we show that the P2X7 receptor was highly expressed in both OCA biopsies and in human OCA cell lines. Studying its activation in SKOV-3 cells, it was found that P2X7 was not a cell death inductor, and that SKOV-3 cells released ATP into the medium. Moreover, when stimulated through the released ATP, the P2X7 receptor mediated ERK and AKT activation, and its antagonism by various means decreased cell viability. All together these results strongly suggested that SKOV-3 cancer cells auto-regulate their proliferative rate through a purinergic system that involved the P2X7 receptor.

MATERIALS AND METHODS

HUMAN SAMPLES AND OVARIAN CANCER CELL LINES

Paraffinized human biopsies were obtained from the Instituto Nacional de Cancerología (INCAN) México following ethical procedures. Clinical histories are deposited in the INCAN archives, and histopathologic diagnoses were determined using international parameters of the World Health Organization Classification of Tumours [Lee et al., 2003].

Ovarian cancer cell lines SKOV-3, CAOV-3, and MM14.Ov were obtained from ATCC, cultured according to ATCC guidelines, and maintained at 37°C in a humidified atmosphere containing 5% CO_2.

IMMUNOHISTOCHEMISTRY

The analysis of paraffinized samples of ovarian biopsies was performed as described in a previous report [Vázquez-Cuevas et al., 2013]. The primary antibody utilized was anti-P2X7 at a dilution of 1:100 (Alomone, Jerusalem, Israel) and the secondary antibody was anti-rabbit HRP diluted 1:100 (Life Technologies, Carlsbad, CA). Labeled tissue was visualized by adding diaminobenzidine substrate; the samples were then stained with hematoxylin and mounted in DABCO (Sigma–Aldrich, St. Louis, MO).

IMMUNOFLUORESCENCE

For immunofluorescence, cell cultures were incubated with 10 μM FM4-64 dye (Life Technologies) in phosphate-buffered saline (PBS, containing in mM: 136 NaCl, 2.7 KCl, 10 Na_2HPO_4, 1.8 KH_2PO_4, pH 7.4) for 20 min, then fixed with 4% paraformaldehyde (PFA) in PBS for 20 min. Immunodetection was performed as described previously [Vázquez-Cuevas et al., 2013]. Both primary (anti P2X7, Alomone) and secondary antibodies (anti rabbit-Alexa Fluor 488, Life Technologies) were added in 1:100 dilutions. The samples were analyzed using confocal fluorescence microscopy (LSM 510, Karl Zeiss, Germany).

DEOXYRIBONUCLEOTIDYL TRANSFERASE NICK END LABELING (TUNEL) AND LACTATE DEHYDROGENASE (LDH) ASSAYS

Apoptotic cell death was assayed by the TUNEL method with the kit *Dead end Fluorometric Assay* (Promega, Madison, WI); for this, cells were cultured on cover slides, fixed in 4% PFA, and processed according to the manufacturer's instructions. Briefly, fixed cells were incubated with labeling buffer containing dUTP-fluorescein and the transferase enzyme; the reaction was stopped by rinsing twice with PBS buffer, and the slides were mounted in VectaShield (Vector Laboratories, Burlingame, CA).

To quantify total cell death, the LDH level in the culture medium was determined with the kit *LDH-Cytotoxicity Colorimetric Assay* (Biovision, San Francisco, CA). For this, cells were cultured in 96-well dishes; after applying a stimulus and incubating for the indicated time, a 10-μl aliquot of culture medium was analyzed according to the manufacturer's instructions. To determine the maximal absorbance value, the same number of lysed cells was assayed for LDH.

REVERSE TRANSCRIPTION AND POLYMERASE CHAIN REACTION

Total RNA from CAOV-3 cells was purified using the guanidine isothiocyanate method, and cDNA was synthesized using 2 μg of

DNase-treated RNA as previously described [Vázquez-Cuevas et al., 2013].

The cDNA was used as template in a polymerase chain reaction (PCR) to amplify a fragment of 1,730 bp (bases 201-1930) from the human P2X7R transcript (NCBI NM_002562.5). The PCR protocol was initiated by holding the temperature for 3 min at 96°C and ended with 5 min at 72°C. The amplification was performed using 30 cycles of 40 s at 96°C, 40 s at 55°C, and 40 s at 72°C.

The sequences of the oligonucleotides were: forward, CGGATC-CAGAGCATGAATTATG and reverse, CAGTAAGGACTCTTGAAGC.

The amplified sequences were subcloned into the pCR4-TOPO vector (Life Technologies). The nucleotide sequence was confirmed by sequencing.

WESTERN BLOT

For analysis of ERK and AKT phosphorylation, cells were cultured in 12-well plates (5×10^4 cells/well). Before each experiment cells were incubated for 12 h in serum-free DMEM; after applying a treatment, cells were scraped in 2× Laemmli buffer (containing: 125 mM Tris–HCl pH 6.8, 140 mM SDS, 30 mM bromophenol blue, 20% glycerol, and 2% 2-mercaptoethanol) and boiled for 10 min. Western blot analysis was performed as previously described [Vázquez-Cuevas et al., 2013]. The primary antibodies utilized were anti-P2X7 1:1000 (Alomone), anti-phosphorylated ERK 1:1,000, anti-phosphorylated AKT 1:1,000, anti-AKT total or anti-ERK total 1:2,000 (Cell Signaling Technology, Danvers, MA), and a HRP-conjugated goat anti-rabbit secondary antibody (dilution 1:10,000; Life Technologies). The immunoreactive proteins were detected by chemiluminescence and autoradiography. Images were analyzed with ImageJ Software (NIH-USA).

$[Ca^{2+}]_i$ DETECTION BY FLUORESCENCE MICROSCOPY AND MECHANICAL STIMULATION

SKOV-3 cells were grown on cover slides. Semi-confluent cultures (70–80%) were loaded with 5 mM Fluo-4/AM (Life Technologies) in Krebs solution (containing in mM: 150 NaCl, 1 KCl, 1 $MgCl_2$, 1.5 $CaCl_2$, 4 glucose, and 10 HEPES, pH 7.4). The cells were placed in a constant-flow recording chamber located in an inverted fluorescence microscope (Olympus IX10). Drugs were applied in the superfusion solution, and responses were recorded for 100 s at a frequency of 3 Hz. Sequences of images were analyzed using ImageJ software (NIH-USA). ATP release evoked by mechanical stimulus was assessed by detecting $[Ca^{2+}]_i$ changes in the absence and presence of apyrase (20 U/ml). For this, cells were loaded with Fluo4-AM (Life Technologies) and monitored as described above. Mechanical stimulation was produced by a jet of Krebs solution ejected through a patch-clamp micropipette for 1–2 s, applying positive pressure of 200–250 hPa; the micropipette was positioned on a particular cell using a micromanipulator while a complete optical field was monitored. Images were analyzed with the software ImageJ.

CELL VIABILITY

To analyze the cell viability, mitochondrial activity of the whole culture was assessed by using the [3-(4,5-dimethylthiazol-2-yl)-5-(3-carboxymethoxyphenyl)-2-(4-sulfophenyl)-2H-tetrazolium salt (MTS) assay (Promega). For this, cells were cultured in 96-well plates in DMEM–10% FBS, and after 24 h they were transferred to serum-free DMEM-F12 for 8 h. After this, an appropriate stimulus was applied, and the cultures were incubated for additional 48 h. Finally, the MTS assay was performed as described by the manufacturer. Results were expressed as fold increase of absorbance relative to unstimulated cells.

TRANSFECTION

For lipofection, 2×10^4 SKOV-3 cells were cultured in 250 μl of DMEM containing 10% FBS and without antibiotic in 48-well dishes until they reached 80–90% confluence. Then a mixture of 1 μl lipofectamine (Life Technologies) and 500 ng of each plasmid in Opti-MEM (Life Technologies) was added to each well; 8 h later the medium was replaced by DMEM/FBS, and the cultures were incubated for 48 h then assayed for viable cells by the MTS method.

BIOTINYLATION OF PLASMA MEMBRANE PROTEINS

Proteins expressed in the plasma membrane of CAOV-3 cells were biotinylated by incubating the cell cultures for 20 min with a 300 μM solution of the membrane-impermeable biotinylation reagent Ez-link Sulfo NHS-LC-LC-Biotin (Thermo Scientific, Waltham, MA) in PBS. Then, total membranes were isolated according to standard procedures [Rangel-Yescas et al., 2012] and then solubilized in TNTE buffer (containing in mM: 50 Tris–HCl pH 7.4, 150 NaCl, 1 EDTA, and 0.1% Triton X-100); an aliquot containing 500 μg of total protein was incubated for 2 h at room temperature with 25 μl agarose beads bound to monomeric avidin (Thermo Scientific), the beads were washed, resuspended in 50 μl of Laemmli solution, and boiled. Expression of the P2X7 receptor was then evaluated by Western blot as described above.

RESULTS

P2X7 RECEPTOR EXPRESSION IN BIOPSIES OF HUMAN OVARIAN TUMORS

The P2X7 receptor was recently shown to be expressed in the human OSE and in some OCA samples [Vázquez-Cuevas et al., 2013]. We extended this analysis to include nine carcinoma samples (pathological descriptions are shown in Table I), and two healthy ovaries as controls.

In the normal ovary, the P2X7 receptor was specifically detected in the OSE (Fig. 1) as a monolayer surrounding the ovary. In all the tumor samples, the P2X7 signal was again detected in the OSE layer, which showed distinct degrees of hypertrophy and hyperplasia, but in addition there was a high level of P2X7 receptor in zones located in the ovarian stroma. Figure 1 illustrates the P2X7 expression in three different biopsies that corresponded to: mucinous, border-line, and endometrial adenocarcinoma tumors, see color image in the electronic version.

ADENOCARCINOMA-DERIVED SKOV-3 CELLS EXPRESS P2X7 RECEPTORS, AND THEIR STIMULATION ELICITS $[Ca^{2+}]_i$ INCREASE

The high-level P2X7 receptor expression in OCA samples might be indicating a role in ovarian cancer. To explore this possibility, P2X7 expression and the effects of its activation were studied in the OCA cell line SKOV-3, which has been extensively characterized and is considered a suitable model for ovarian epithelium-derived cancer cells [Auersperg et al., 2001].

TABLE I. Characteristics of Tumors Analyzed in This Study and P2X7 Expression

Sample number	Patient age	Histopathologic diagnosis	P2X7 abundance
IC09-252-1	43	Borderline serous tumor, stage 1b	++
IC11-11595	43	Clear cell carcinoma	++
IC11-3652-12	57	Clear cell carcinoma	+++
IC09-917-12	30	Endometrioid G1-type carcinoma	++++
IC11-7381	53	Endometrioid G3-type carcinoma	+++
IC11-9294-16	45	Endometrioid G2-type carcinoma	+++
IC11-12697-11	51	Endometrioid G2-type carcinoma	++
IC11-12062-7	41	High-grade papillary serous carcinoma	+++
ICOD8-12310-13	73	Mucinous adenocarcinoma	++++
4340	55	Non-cancerous	+
4672	65	Non-cancerous	+

Expression of the P2X7 receptor in SKOV-3 cells was confirmed by RT-PCR, Western blot, and immunocytochemistry [Vázquez-Cuevas et al., 2013]. To substantiate these findings, P2X7 was localized in the membrane by immunocytochemistry and confocal microscopy; the cells were stained with FM4-64, a dye that specifically labels the plasma membrane, and with DAPI to mark the nuclei. The result of this analysis is illustrated in Figure 2A. Three panels are shown for typical cell images; in the first, FM4-64 and DAPI were visualized through the red and blue channels, respectively. As noted in the orthogonal projection (OP image), the membrane and nucleus were effectively resolved. In the middle panel, a similar image was obtained when P2X7 was labeled with the specific primary antibody and the secondary antibody conjugated with Alexa Fluor 488 in green; P2X7 label remained in close apposition above to the nucleus, and it strongly co-localized with the plasma membrane, as shown in the last panel where all the channels were merged, see color image in the electronic version. Thus, P2X7 was localized mainly in a membrane area adjacent to the nucleus.

To study the effects produced by P2X7 receptor activation, SKOV-3 cells were analyzed using fluorescence microscopy to monitor changes in $[Ca^{2+}]_i$ during P2X7 stimulation by BzATP, a specific agonist.

Stimulation of SKOV-3 cells by BzATP induced a transient $[Ca^{2+}]_i$ increase (Fig. 2B, left panel). The response was concentration dependent with an $EC_{50} = 494 \pm 77$ nM (Fig. 2B, right graph) and a maximal effect of $200 \pm 6\%$ compared to the basal level. To further test the specificity of the signal for P2X7 activation, SKOV-3 cells were preincubated with 10 μM A438079, a selective P2X7 antagonist, and then stimulated by co-applying 10 μM BzATP. As shown in Figure 2C (upper panel), treatment with the antagonist abolished the Ca^{2+} increase response; however, after 7 min of washing with normal external solution, the same cells were able to respond to BzATP alone. Similar experiments in which BzATP was replaced by 10 μM ATP, a concentration that does not activate the P2X7 receptor, generated a similar $[Ca^{2+}]_i$ increase; however, this increase was not affected by 10 μM A438079 (Fig. 2C, lower panel). Thus, the $[Ca^{2+}]_i$ increase induced by ATP was $183 \pm 7.9\%$ and $169 \pm 8.5\%$ of basal with or

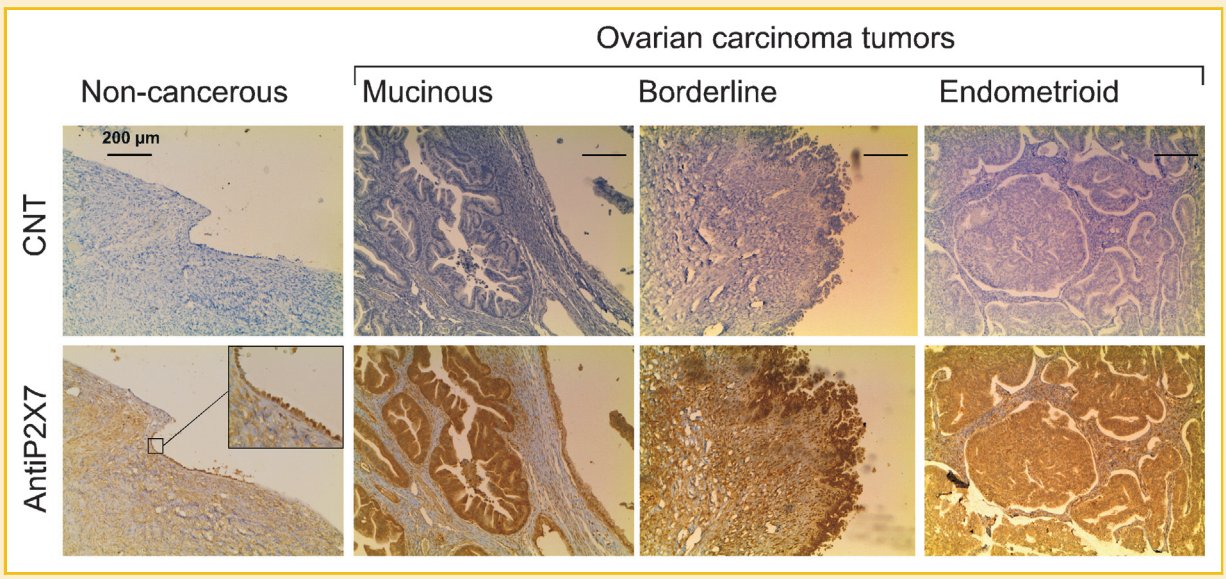

Fig. 1. Immunocytochemical detection of the P2X7 receptor in normal tissue and human ovarian carcinoma. Biopsies from the ovary of non-cancerous and carcinoma tissue were collected, processed, and stained with hematoxylin and/or labeled with anti-P2X7 antibody that was revealed by the horseradish peroxidase and diaminobenzidine method (brown signal). Images corresponded to 10-μm slices visualized by light microscopy, see color image in the electronic version.

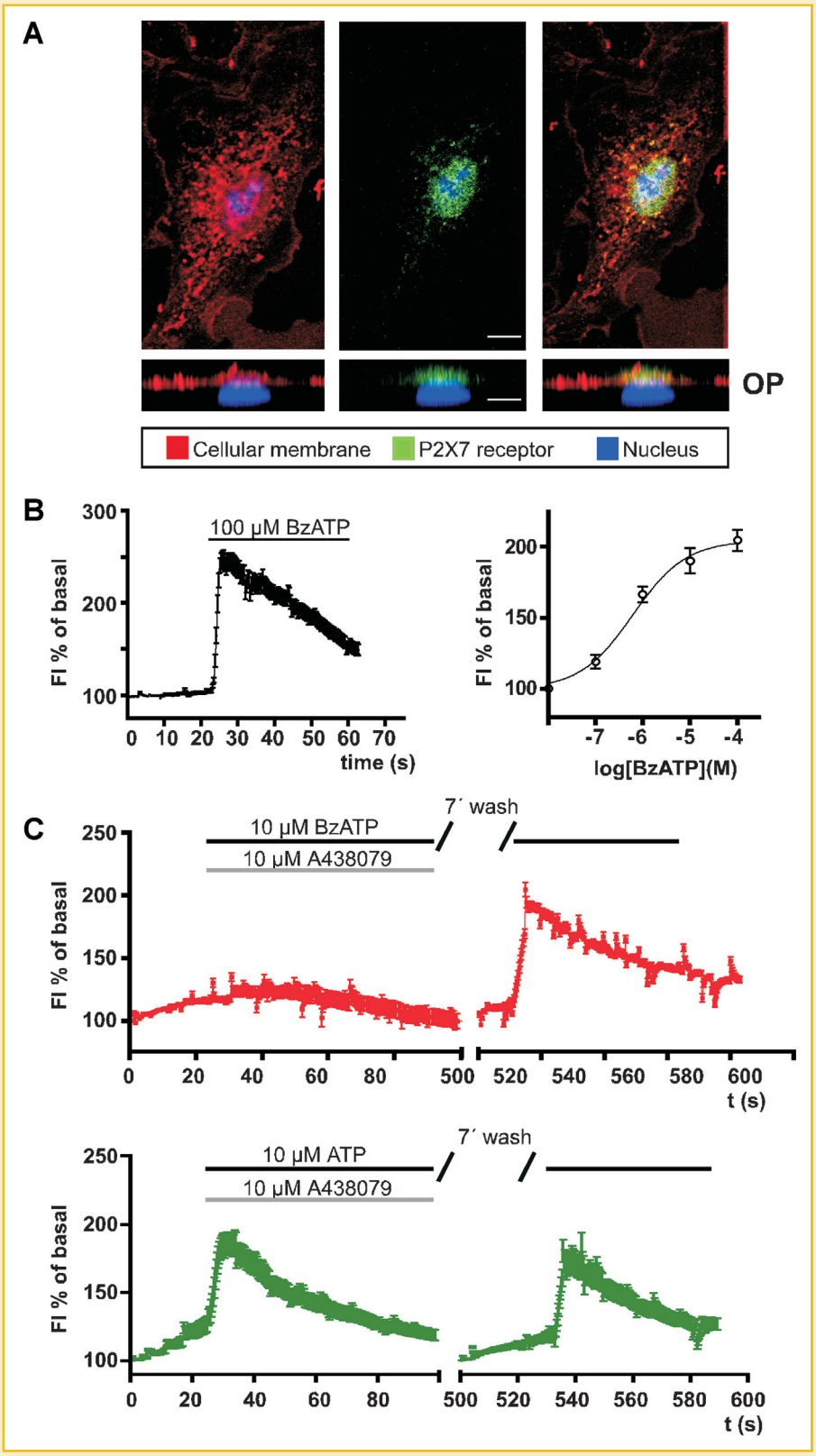

Fig. 2. Subcellular localization and functional expression of P2X7 in SKOV-3. A: Immunofluorescence images of SKOV-3 cells were stained with: FM4-64 dye (in red) for plasma membrane, secondary antibody coupled to Alexa fluor 488 (green) for P2X7 receptor, and DAPI (blue) for nucleus. Left panel illustrates plasma membrane and the middle panel shows localization of P2X7 labeling, both with respect to the nucleus; the right panel is the corresponding merged image, see color image in the electronic version. Images include orthogonal projections (OP, bottom); calibration bar corresponds to 10 μm. B: $[Ca^{2+}]_i$ increase induced by 100 μM BzATP (left) and dose–response relationship for BzATP (right). C: Incubation with the antagonist A438079 prevented the BzATP-induced increase of $[Ca^{2+}]_i$; a wash period restored the response (upper panels); the antagonist did not affect the response induced by 10 μM ATP (lower panels).

without A438079, respectively (50 cells from five independent cultures). These results supported the idea that the P2X7 receptors expressed in the membrane of SKOV-3 cells were functional.

P2X7 RECEPTOR ACTIVATION DID NOT INDUCE CELL DEATH IN SKOV-3 CELLS

To determine if P2X7 activation induced apoptosis in SKOV-3 cells, the cultures were incubated for 24 h with 50 μM BzATP, and genomic DNA fragmentation was then evaluated by TUNEL. In treated SKOV-3 cells (three independent preparations), no positive signal indicating apoptosis was detected; as a positive control, cells were treated in parallel with 50 μM staurosporine (Fig. 3A), which always produced apoptosis. Moreover, the non-transformed MM14.0v epithelial-like cell line that also expressed the P2X7 receptor [Vázquez-Cuevas et al., 2013] was sensitive to BzATP and became apoptotic after 24 h of stimulation (Fig. 3B), strongly suggesting that the inability of BzATP to induce cell death was specific for SKOV-3 cells.

In order to know whether or not BzATP could induce cell death through a non-apoptotic mechanism, SKOV-3 cells were incubated with 50 μM BzATP for 24 h, and the LDH released was measured. The result showed that BzATP treatment did not induce LDH release (Fig. 3C), indicating that P2X7 activation was unable to induce SKOV-3 cell death.

P2X7 ACTIVATION IN SKOV-3 INDUCED PHOSPHORYLATION OF ERK AND AKT KINASES

There exists evidence supporting the notion that the P2X7 receptor participates in controlling proliferation of normal and malignant cells [Di Virgilio et al., 2009]. In order to test whether or not P2X7 activation induces activation of kinases related to proliferative or survival pathways in SKOV-3 cells, a human phospho-MAPK array was used to evaluate the effect of treating cells for 30 min with 10 μM BzATP on the phosphorylation levels of Jnk, ERK, p38, AKT, and GSK3; the result showed that BzATP induced an increase in phosphorylation of ERK proteins and a minor effect on JNK proteins (Fig. 4).

ERK protein activation is closely associated with cell cycle regulation and proliferation induction [Chambard et al., 2007], and its modulation is obviously relevant in cancer progression [Poulikakos and Solit, 2011]. In order to analyze specifically the BzATP-induced ERK phosphorylation in SKOV-3, cell cultures were stimulated with the agonist, and ERK phosphorylation changes were quantified. ERK phosphorylation increased to $150 \pm 30\%$ of the basal level when cells were stimulated with 10 μM BzATP (Fig. 5A); this effect was completely blocked by A438079 (10 μM), indicating the specific involvement of P2X7 in the phenomenon (Fig. 5A, left panel).

ERK phosphorylation elicited by BzATP was concentration dependent; it had an EC_{50} of 44 ± 3 nM (Fig. 5A, center panel) and reached a maximum of $305 \pm 20\%$ of the basal level. The response elicited by 10 μM BzATP was detectable as early as 5 min after agonist addition, reached a peak at 15 min, and remained elevated for the entire 120 min evaluated (Fig. 5A, right panel) (four independent cultures, each in duplicate).

Due to the importance of AKT in cancer we performed a more detailed study to detect if the stimulation of SVOV-3 cells with

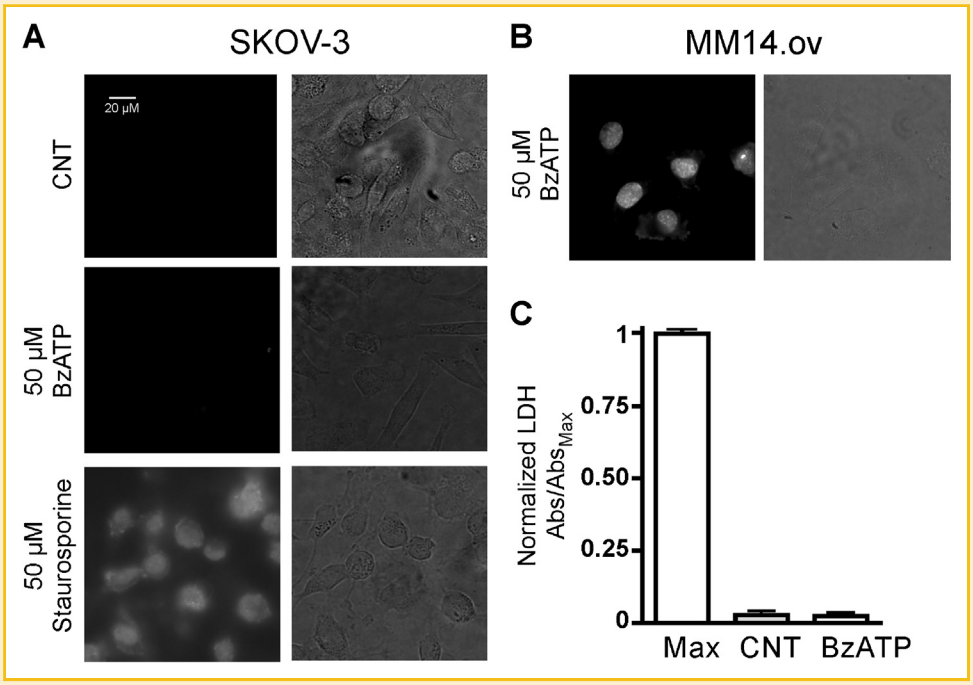

Fig. 3. BzATP did not induce apoptosis in SKOV-3 cells. A: Induction of apoptotic cell death was evaluated by TUNEL in SKOV-3 cells treated with 50 μM BzATP for 24 h; as positive control, cells were treated in parallel with 100 nM staurosporine. B: Similar assay was performed in MM14.0v, a non-cancerous, epithelial-like cell line. C: LDH concentration, to assess total cell death in the culture medium of SKOV-3 cells stimulated or not (CNT) by 50 μM BzATP for 24 h; the maximum LDH level (Max) was determined by lysis of an equivalent number of cells.

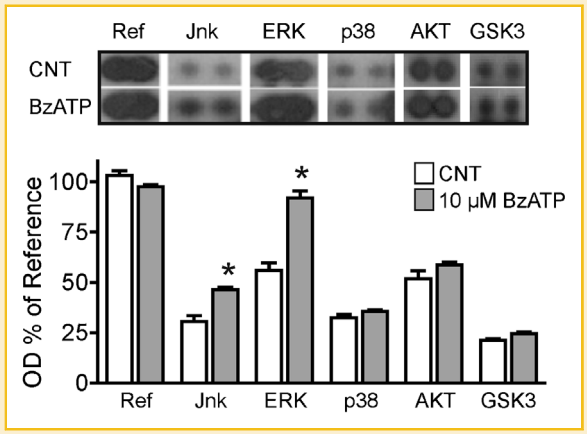

Fig. 4. BzATP modulated kinase phosphorylation in SKOV-3. Phosphorylation degree of JNK, ERK, p38, AKT, and GSK3 was detected in SKOV-3 cells treated or not (CNT) with 10 μM BzATP using a commercial phospho-kinase array. Ref, corresponds to an internal reference for the assay. *$P < 0.05$ vs. CNT.

BzATP induces an increase in pAKT levels. We used Western blot assays and detected pAKT with a specific antibody (Cell Signaling Technology); this method was more sensitive than the phospho-MAPK array. BzATP induced an increase in the AKT phosphorylation level, with an EC_{50} of 1.27 ± 0.5 nM (Fig. 5B, center panel); this effect was abolished by preincubation with A438079 (Fig. 5B, left panel). AKT phosphorylation increased within the first 5 min of stimulation and was maintained for at least 2 h (Fig. 5B, right panel). Thus, these observations suggested that AKT was a downstream target of P2X7 activation in SKOV-3 cells.

MECHANICAL STIMULATION OF SKOV-3 CELLS SEEMED TO GENERATE ATP-ELICITED RESPONSES

From the results described above, it was also evident that both ERK and AKT had a high basal level of phosphorylation (see Fig. 5). It is well known that purinergic communication serves as an important paracrine messenger in diverse cellular systems [Burnstock, 2007; Corriden and Insel, 2010]; therefore, ATP released from the SKOV-3 cells might affect ERK and AKT phosphorylation by acting as a local modulator.

As an indirect test for possible ATP release, SKOV-3 cells were mechanically stimulated while monitoring their $[Ca^{2+}]_i$ response. For this, a brief jet of Krebs solution was applied through a micropipette onto one cell of a semiconfluent culture loaded with Fluo4-AM fluorescent dye, and the response was analyzed. As illustrated in Figures 6A and B, mechanical stimulation induced a significant increase in $[Ca^{2+}]_i$ to $122 \pm 15\%$ of the basal level (Fig. 6B, black circles) in all cells of a particular field observed, since the response propagated among the cells as a wave that always started in the stimulated cell. Incubation with apyrase (20 U/ml) for 5 min completely inhibited the response ($91 \pm 2.55\%$ of basal) induced by the mechanic stimulus (Fig. 6B, gray circles). A similar increase was observed in 53% of the preparations from 15 different cultures, and in all cases the effect was completely abolished by apyrase. This strongly suggested that the $[Ca^{2+}]_i$ increase was mediated mainly by ATP release. Thus, cell cultures were incubated with apyrase, and ERK and AKT phosphorylation as well as viable cells were evaluated.

AKT phosphorylation was measured after 6 and 12 h (Fig. 6C) in the presence of apyrase (10 U/ml), and the pAKT level decreased to $50 \pm 16.1\%$ and $67.9 \pm 3.7\%$ of the control, respectively. Also, pERK (Fig. 6D) decreased after 6 h of incubation ($56.5 \pm 12.4\%$ compared to the control), and showed recovery at 12 h ($90.7 \pm 7.7\%$). Moreover, after 48 h apyrase caused a decrease in cell viability to $90.3 \pm 1.4\%$ versus the control (Fig. 6E). Our data showed that ATP present in the extracellular medium modulated cell growth and the levels of both pAKT and pERK.

CELL VIABILITY OF SKOV-3 CELLS WAS MODULATED BY A P2X7 RECEPTOR ANTAGONIST AND BY TRANSFECTION OF THE E496A VARIANT OF THE P2X7 RECEPTOR

Next, we evaluated the involvement of basal P2X7 activity on SKOV-3 cell viability, as measured by the MTS method; for this, cells were treated with a specific antagonist of P2X7, and cell viability was evaluated at 48 h. In the presence of 1 or 10 μM AZ10606120, cell viability was reduced to $87.8 \pm 1.6\%$ and $70.1 \pm 8.9\%$, respectively, relative to the control culture (Fig. 7A); similar effects were observed using oxidized ATP (oATP) as antagonist.

To further support the conclusion that reduction in cell proliferation depended on P2X7 receptor activity, SKOV-3 cells were transfected with a plasmid containing the P2X7 receptor mutant E496A [Gu et al., 2001], a dominant negative variant (Fig. 7B), and viable cells were measured 48 h later. The results of three independent transfections, each in triplicate, showed that cell viability was reduced to $76.5 \pm 4.89\%$. Both results, the P2X7 antagonist effect and the mutant E496A transfection, strongly suggested that P2X7 signaling, stimulated by ATP release, contributed to the growth SKOV-3 OCA cells.

P2X7 EXPRESSION IN CARCINOMA CELL LINE CAOV-3

CAOV-3 cells were analyzed to explore whether or not a different cell line derived from OCA expressed functional P2X7 receptors. For this, a 1,730-bp fragment of the P2X7 transcript was amplified by PCR from cDNAs derived from CAOV-3 cells (Fig. 8A), and sequencing confirmed the identity of this amplicon. In samples of plasmatic membrane proteins that had been biotinylated and isolated by avidin affinity P2X7 was detected by Western blotting using an antibody against its carboxy-terminus and compared with SKOV-3 samples (Fig. 8B).

Similar to SKOV-3 cells, in CAOV-3 cells BzATP increased ERK phosphorylation in a dose-dependent manner; an increase in ERK phosphorylation was evident within the first 15 min of stimulation and was maintained for at least 2 h (Fig. 8C).

Also similar to the observations in SKOV-3, application of BzATP did not induce CAOV-3 cell death, as evidenced by the LDH release assay (Fig. 8D), and the P2X7 antagonist oATP (at 1 and 10 μM) decreased cell viability (Fig. 8E).

Thus, the effects observed in SKOV-3 and attributed to P2X7 activation were reproduced in CAOV-3 cells, suggesting that P2X7 expression and actions were a common characteristic of carcinoma cells.

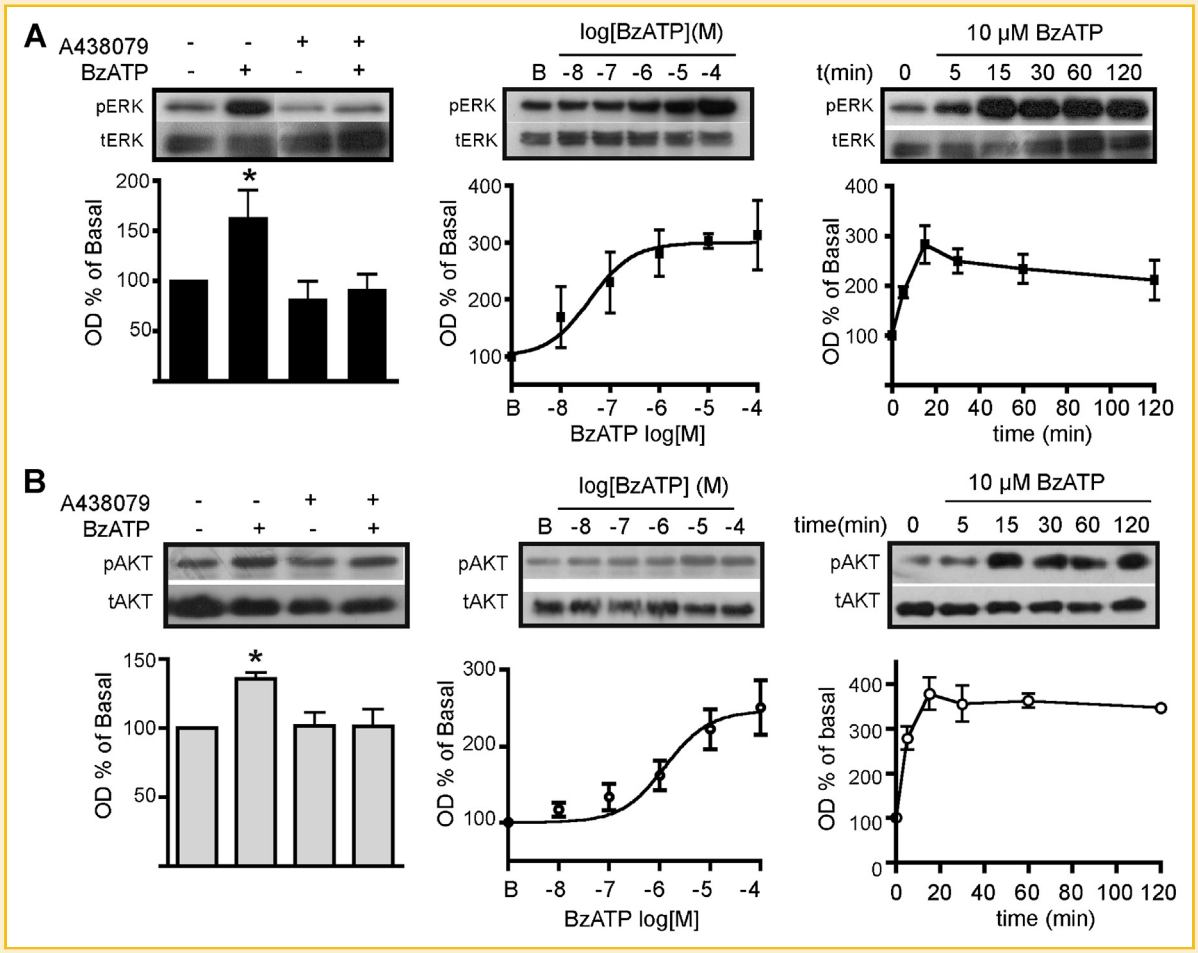

Fig. 5. BzATP-induced ERK and AKT phosphorylation through P2X7-specific activation that was dose dependent and Ca^{2+} independent. A: ERK phosphorylation was detected by Western blot in SKOV-3 cells exposed to treatment or not with BzATP (10 μM) and/or A438079, a selective P2X7 antagonist (10 μM), left panel; (*$P < 0.05$ vs. control). Dose–response curve for pERK induced by BzATP (center panel), and time-course of ERK phosphorylation in cells stimulated with 10 μM BzATP (right panel). B: addition of 10 μM BzATP for 15 min induced AKT phosphorylation, and this was blocked by the P2X7 antagonist A438079 (10 μM), left panel;(*$P < 0.05$ vs. control). Dose–response relationship of AKT phosphorylation induced by BzATP (center panel), and time course of AKT phosphorylation induced by 10 μM BzATP (right panel).

DISCUSSION

Here, we studied different types of human OCA to evaluate expression of the P2X7 receptor and the effects of its activation. We found that: (i) Normal tissue and carcinoma expressed the P2X7 receptor protein, however, the carcinoma biopsies shown an elevated level of P2X7 protein; (ii) In carcinoma cell lines, specific P2X7 activation by BzATP evoked increases of $[Ca^{2+}]_i$ and ERK and AKT phosphorylation; (iii) P2X7 receptor activation did not induce cell death; (iv) The basal level of pERK and pAKT was downregulated by incubation with apyrase, suggesting ATP release; (v) Evidence for ATP release was found in SKOV-3 cells subjected to mechanical stimulation, which produced an increase in $[Ca^{2+}]_i$; and (vi) Pharmacological antagonism and expression of variant dominant negative of P2X7 receptor decreased the levels of pERK and pAKT as well as cell viability.

In control human biopsies the immunoreactive signal for P2X7 was mainly localized in the OSE, observed as a monolayer covering the ovary surface; this cell type has been hypothesized as the origin of OCA [Auersperg et al., 2001; Murdoch and McDonnel, 2002]. In carcinoma biopsies, the epithelium showed major changes in organization, and it displayed hypertrophy, hyperplasia, and stratification. Strong P2X7 receptor expression was detected in this modified epithelium in all classes of carcinoma examined. Biopsies also showed extensive zones in the region of the stroma with high immunoreactivity to P2X7 receptor.

Thus, P2X7 receptor expression in human cancer samples raises the possibility that in the pathological context, the P2X7 receptor does not act as an inductor of apoptosis but instead; it has a role in cell proliferation. Thus, we have evaluated with more detail the consequences of P2X7 activation in the OCA cell lines SKOV-3 and CAOV-3.

Previously we have shown that the SKOV-3 cell line express P2X7 protein [Vázquez-Cuevas et al., 2013]; here, this observation was extended by determining its subcellular localization and whether or not P2X7-specific activation was able to modify $[Ca^{2+}]_i$. It was

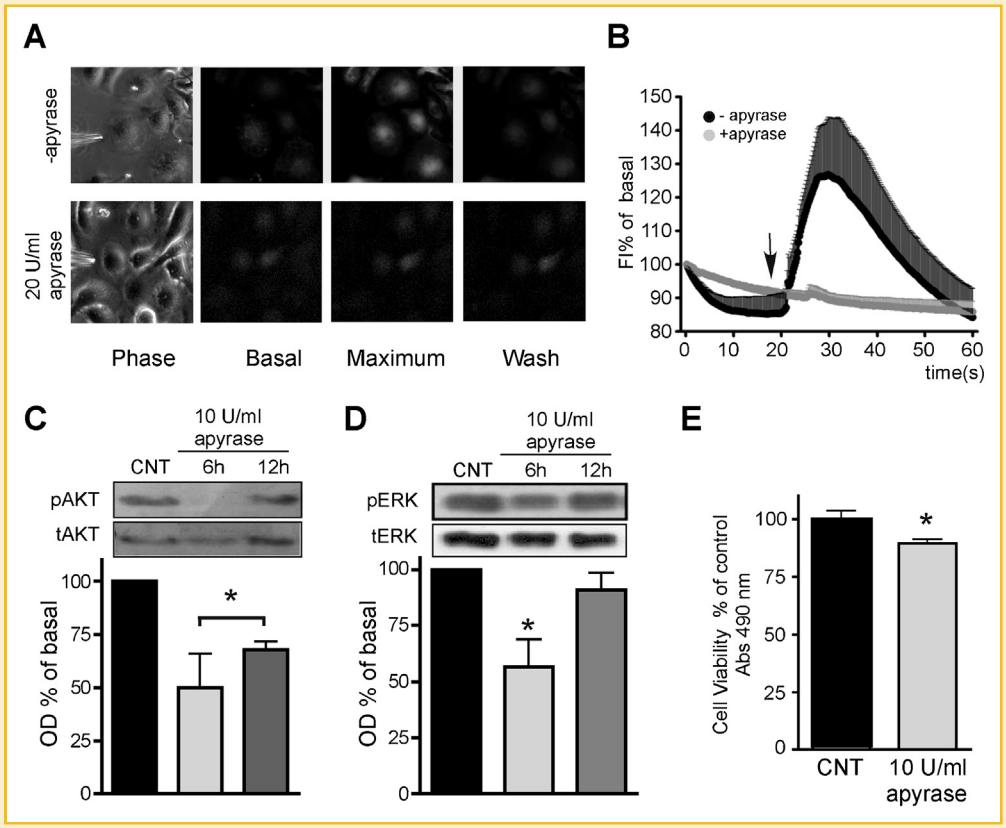

Fig. 6. Mechanical stimulation of SKOV-3 induced a $[Ca^{2+}]_i$ increase that was inhibited by apyrase; this nucleotidase also modulates the phosphorylation state of AKT and ERK and the cell viability. A: Changes in fluorescence were recorded for 60 s in SKOV-3 cells loaded with Fluo-4-AM, and a single cell was stimulated with a jet of Krebs solution. The protocol was carried out either in the presence or absence of 20 U/ml apyrase. B: Graph of a typical experiment; the arrow indicates the time of mechanical stimulation (pulse of 2 s), in the presence (gray circles) or not of apyrase (black circles), each data point represents the mean and standard error of 63 cells with apyrase and 79 control cells. Phosphorylation level of AKT (C) and ERK (D) was evaluated after 6 and 12 h of incubation with 10 U/ml apyrase. E: SKOV-3 cells were incubated 48 h in the presence of 10 U/ml apyrase (FBS-free culture medium), and viable cells evaluated by the MTS assay and compared those in an untreated culture (CNT) (*$P < 0.05$ vs. CNT).

observed by immunofluorescence that P2X7 co-localized with the signal of FM4-64, a dye specific for the plasma membrane, strongly suggesting that the receptor was located mainly within a restricted area of the plasma membrane in close apposition to the nucleus. An increase in Ca^{2+} concentration in the immediate vicinity of the nucleus might have important consequences for regulation of gene transcription and cell proliferation [Rodrigues et al., 2007]. By monitoring changes in $[Ca^{2+}]_i$ we also showed that the P2X7 receptor is functional since its specific activation by BzATP induced a $[Ca^{2+}]_i$ increase that was blocked by the specific antagonist A438079.

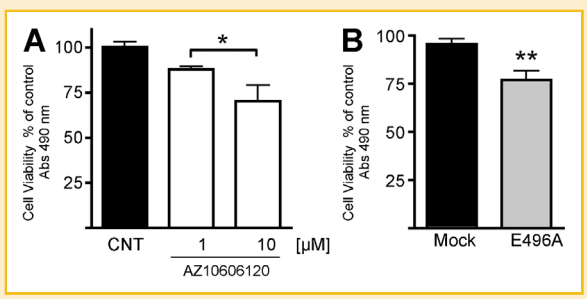

Fig. 7. P2X7 antagonist or SKOV-3 transfection with a dominant negative P2X7 variant regulated cell viability. Viable cells were quantitated after 48 h by the MTS method, in A) SKOV-3 cells treated or not (CNT) with AZ10606120 (either 1 or 10 μM), and in B) cells transfected or not (mock) with the dominant negative P2X7 mutant E496A. (*$P < 0.05$ vs. CNT; **$P < 0.05$ vs. Mock; Student's *t*-test).

Thus, this study was focused on cellular responses induced by specific stimulation of the P2X7 receptor, and the first goal was to determine the ability of P2X7 to induce cell death. The results obtained using both LDH and TUNEL assays indicated that P2X7 activation did not induce cell death or DNA fragmentation in SKOV-3 cells.

It has been described that the pharmacological stimulation of the P2X7 receptor induces cell death in various cellular models; the main mechanism for this response involves an induction of cytosolic Ca^{2+} overload leading to activation of the mitochondrion-dependent apoptosome [Coddou et al., 2011]. Thus, the inability of BzATP to induce cell death in SKOV3 and CAOV3 lines may be related to alterations in one or various cellular components that participate in this mechanism. First, it may be related to expression of variants of the P2X7 receptor, some of which present phenotypes of diminished or loss of function (Adinolfi et al., 2010); however, reduced

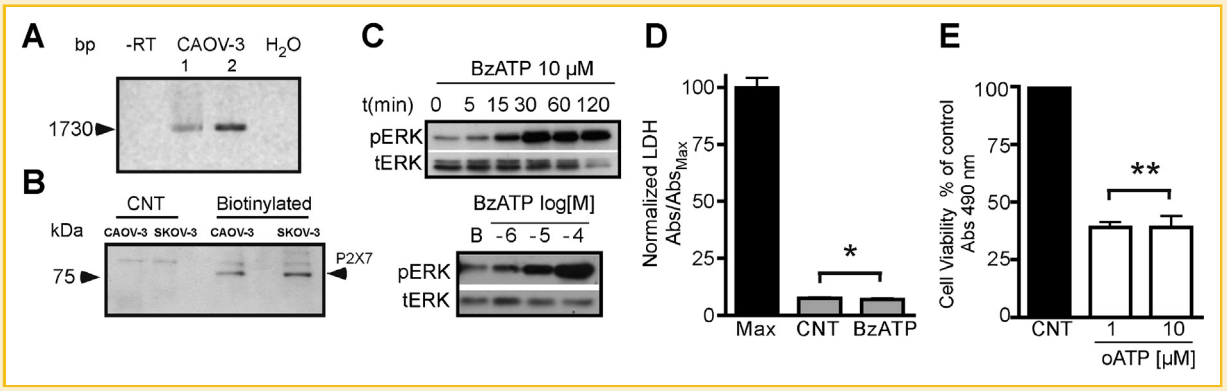

Fig. 8. P2X7 expression and function in CAOV-3 cell line. A) RT-PCR amplification of a fragment of P2X7 from two samples of CAOV-3 cells (-RT, control without reverse transcription; H_2O, control with the reaction mix without template); B) Western blot of P2X7 in biotin-tagged membrane proteins isolated by affinity to avidin in the cell lines CAOV-3 and as positive control SKOV-3; C)Time course (upper panel) and dose-response curve (lower panel) of ERK phosphorylation induced by BzATP; D) LDH level in the culture medium of CAOV-3 cells stimulated or not (CNT) by 50 µM BzATP for 24 h; maximum (Max) was determined by lysis of an equivalent number of cells, and E) Number of viable cells estimated by MTS assay of CAOV-3 cells incubated for 48 h with oxidized ATP (oATP) (*$P < 0.05$ vs. Max, **$P < 0.05$ vs. CNT; Student's t-test).

expression of accessory proteins, like pannexin 1, that interact with the P2X7 receptor can account for this insensitivity to induction of P2X7-dependent cell death. Moreover, the resistance to cell death should be potentiated by multidrug-resistance mechanisms present in cancer cells. Detailed studies of these mechanisms are necessary to define if P2X7 might be considered a tumor-suppressor gene.

Instead of cell death, P2X7 activation induced a robust activation of ERK and a minor but consistent activation of AKT. ERK and AKT phosphorylation through P2X7 activation have been reported in distinct cell types [Panenka et al., 2001; Bradford and Soltoff, 2002; Jacques-Silva et al., 2004; Stefano et al., 2007; Ortega et al., 2009]; both kinases are signals for cell growth and survival and are involved in cancer mechanisms [Altomare and Testa, 2005; Hers et al., 2011; Poulikakos and Solit, 2011; Dobbin and Landen, 2013]. In both cell lines analyzed in this study, phosphorylation of ERK was induced in a dose-dependent manner and had a time-course similar to that described in other cell types [Stefano et al., 2007]. Also, in SKOV-3 cells ERK and AKT activation was abolished by A438079, a specific P2X7 antagonist, indicating that these responses were specifically induced by P2X7 activity and suggesting a role for this receptor in cell growth.

Phosphorylated forms of both ERK and AKT were present at detectable levels in intact cultures. Considering that ATP is an autocrine–paracrine cellular messenger [Corriden and Insel, 2010], and that a broad variety of cellular systems are able to release ATP spontaneously and/or by mechanical stimulation [Sauer et al., 2000; Selzner et al., 2004; Saldaña et al., 2009; Corriden and Insel, 2010], we tested the hypothesis that the high constitutive levels of pERK and pAKT were related to ATP release into the medium by the SKOV-3 cells.

The experiments showed that a mechanical stimulus induced a robust rise in the intracellular Ca^{2+} level; this increase was completely abolished by the presence of apyrase, strongly supporting the idea that ATP mediated the response. The results suggested that the transmitter was released from the stimulated cell, and the signal propagated to neighboring cells.

A continuous effect of the ATP released by SKOV-3 cells was further supported by evidence demonstrating that apyrase also reduced the cell viability, measured as the mitochondrial activity of the culture, this observation is relevant because has been shown that MTS assay correlates with cellular proliferation [Kanemura et al., 2009]. The reduced rate of SKOV-3 growth was concomitant with down-regulation of ERK and AKT protein phosphorylation. Thus, ATP release might be an important signal for trophic control; in this sense it has been shown that the ATP concentration in the microenvironment of induced tumors is on the order of hundreds of mM [Pellegatti et al., 2008], suggesting that ATP release from cancer cells, acting through P2 receptors, contributes to a positive feedback for tumor growth.

Finally, we explored whether P2X7 activation through paracrine/autocrine mechanisms influenced the cell viability in SKOV-3 cells. The evidence found supported this notion; it was observed that the antagonist AZ10606120 consistently reduced growth compared to control cultures, suggesting that P2X7 stimulation had a positive modulator role on proliferation. This agreed with the demonstration that transfection of E496A, the dominant negative variant of P2X7, into SKOV-3 cells also reduced cell viability. These results suggested that P2X7 activity promoted SKOV-3 growth, probably as a result of the action of ATP released by the cells into the medium.

We also demonstrated that the CAOV-3 OCA cell line also expresses P2X7 receptor, and its activation generated an increase of $[Ca^{2+}]_i$ as well as induction of ERK phosphorylation, whereas an selective antagonist reduced the total mitochondrial activity of the cell culture, all of these effects were similar to those described in SKOV-3 cells and might be of general occurrence among OCA cells.

In summary, the results presented strongly suggest that the P2X7 receptor is an important element of autocrine-paracrine communication involved in self-sustained tumor growth. This also indicates that expression of the P2X7 receptor in epithelial ovarian cancer represents a potential diagnostic marker and therapeutic target.

ACKNOWLEDGMENTS

This work was supported by Consejo Nacional de Ciencia y Tecnología, México [166725 to F.G.V.-C.], by scholarships to A.S. M.-R. [number 369701], L.R.-M. [number 229134], and C.C.-G. [number 18837] and by Programa de Apoyo a Proyectos de Investigación e Innovación Tecnológica UNAM, México [IN205114 and IA200112 to F.G.V.-C. and IN205312 to R.O.A.]. We are grateful to Dr. Dorothy D. Pless for editing the manuscript. Also, we acknowledge technical assistance by Mr. Horacio Leyva, Ing. Elsa Nydia Hernández Ríos, Ing. Alberto Lara Rubalcava, MVZ Martín García Servín, and Q. Leonor Casanova Rico.

REFERENCES

Adinolfi E, Cirillo M, Woltersdorf R, Falzoni S, Chiozzi P, Pellegatti P, Callegari MG, Sandonà D, Markwardt F, Schmalzing G, Di Virgilio F. 2010. Trophic activity of a naturally occurring truncated isoform of the P2X7 receptor. FASEB J 24:3393–3404.

Adinolfi E, Raffaghello L, Giuliani AL, Cavazzini L, Capece M, Chiozzi P, Bianchi G, Kroemer G, Pistoia V, Di Virgilio F. 2012. Expression of P2X7 receptor increases in vivo tumor growth. Cancer Res 72:2957–2969.

Altomare DA, Testa JR. 2005. Perturbations of the AKT signaling pathway in human cancer. Oncogene 24:7455–7464.

Arellano RO, Garay E, Vázquez-Cuevas FG. 2009. Functional interaction between native G protein-coupled purinergic receptors in *Xenopus* follicles. Proc Natl Acad Sci USA 106:16680–16685.

Arellano RO, Martínez-Torres A, Garay E. 2002. Ionic currents activated via purinergic receptors in the cumulus cell-enclosed mouse oocyte. Biol Reprod 67:837–846.

Auersperg N, Wong AS, Choi KC, Kang SK, Leung PC. 2001. Ovarian surface epithelium: Biology, endocrinology, and pathology. Endocr Rev 22:255–288.

Baricordi OR, Ferrari D, Melchiorri L, Chiozzi P, Hanau S, Chiari E, Rubini M, Di Virgilio F. 1996. An ATP-activated channel is involved in mitogenic stimulation of human T lymphocytes. Blood 87:682–690.

Bradford MD, Soltoff SP. 2002. P2X7 receptors activate protein kinase D and p42/p44 mitogen-activated protein kinase (MAPK) downstream of protein kinase C. Biochem J 366:745–755.

Burnstock G. 2007. Physiology and pathophysiology of purinergic neurotransmission. Physiol Rev 87:659–797.

Chambard JC, Lefloch R, Pouysségur J, Lenormand P. 2007. ERK implication in cell cycle regulation. Biochim Biophys Acta 1773:1299–1310.

Coddou C, Yan Z, Obsil T, Huidobro-Toro JP, Stojilkovic SS. 2011. Activation and regulation of purinergic P2X receptor channels. Pharmacol Rev 63:641–683.

Cormio G, Maneo A, Parma G, Pittelli MR, Miceli MD, Bonazzi C. 1995. Central nervous system metastases in patients with ovarian carcinoma, a report of 23 cases and a literature review. Ann Oncol 6:571–574.

Corriden R, Insel PA. 2010. Basal release of ATP: an autocrine-paracrine mechanism for cell regulation. Sci Signal 3:re1.

Coutinho-Silva R, Persechini PM, Bisaggio RD, Perfettini JL, Neto AC, Kanellopoulos JM, Motta-Ly I, Dautry-Varsat A, Ojcius DM. 1999. P2Z/P2X7 receptor-dependent apoptosis of dendritic cells. Am J Physiol 276:C1139–C1147.

Di Virgilio F, Chiozzi P, Falzoni S, Ferrari D, Sanz JM, Venketaraman V, Baricordi OR. 1998. Cytolytic P2X purinoceptors. Cell Death Differ 5:191–199.

Di Virgilio F, Ferrari D, Adinolfi E. 2009. P2X(7): A growth-promoting receptor-implications for cancer. Purinergic Signal 5:251–256.

Dobbin ZC, Landen CN. 2013. The importance of the PI3K/AKT/MTOR pathway in the progression of ovarian cancer. Int J Mol Sci 14:8213–8227.

Gu BJ, Zhang W, Worthington RA, Sluyter R, Dao-Ung P, Petrou S, Barden JA, Wiley JS. 2001. A Glu-496 to Ala polymorphism leads to loss of function of the human P2X7 receptor. J Biol Chem 276:11135–11142.

Hanahan D, Weinberg RA. 2011. Hallmarks of cancer: The next generation. Cell 144:646–674.

Hers I, Vincent EE, Tavaré JM. 2011. Akt signalling in health and disease. Cell Signal 23:1515–1527.

Jacques-Silva MC, Rodnight R, Lenz G, Liao Z, Kong Q, Tran M, Kang Y, Gonzalez FA, Weisman GA, Neary JT. 2004. P2X7 receptors stimulate AKT phosphorylation in astrocytes. Br J Pharmacol 141:1106–1117.

Kanemura Y, Mori H, Kobayashi S, Islam O, Kodama E, Yamamoto A, Nakanishi Y, Arita N, Yamasaki M, Okano H, Hara M, Miyake J. 2009. Evaluation of in vitro proliferative activity of human fetal neural stem/progenitor cells using indirect measurements of viable cells based on cellular metabolic activity. J Neurosci Res 69:869–879.

Lee KR, Russell P, Tavassoli FA, Buckley CH, Prat J, Pisani P, Dietel M, Schwartz P, Gersell DJ, Goldgar DE, Karseladze AI, Silva E, Hauptmann S, Caduff R, Rutgers J, Kubik-Huch RA. 2003. Surface epithelial-stromal tumours. In: Tavassoli FA, Teville P,editor. Pathology and genetics of tumors of the breast and female genital organs. Lyon, France: World Health Organization Classification of Tumours.

Li X, Qi X, Zhou L, Fu W, Abdul-Karim FW, Maclennan G, Gorodeski GI. 2009. P2X(7) receptor expression is decreased in epithelial cancer cells of ectodermal, uro-genital sinus, and distal paramesonephric duct origin. Purinergic Signal 5:351–368.

Li X, Zhou L, Feng Y, Abdul-Karim FW, Gorodeski GI. 2007. The $P2X_7$ receptor: A novel biomarker of uterine epithelial cancers. Cancer Epidemiol Biomarkers Prev 15:1906–1913.

Munkarah AR, Hallum AV, III, Morris M, Burke TW, Levenback C, Atkinson EN, Wharton JT, Gershenson DM. 1997. Prognostic significance of residual disease in patients with stage IV epithelial ovarian cancer. Gynecol Oncol 64:13–17.

Murdoch WJ, McDonnel AC. 2002. Roles of the ovarian surface epithelium in ovulation and carcinogenesis. Reproduction 123:743–750.

Nakajima EC, Van Houten B. 2012. Metabolic symbiosis in cancer: Refocusing the Warburg lens. Mol Carcinog 52:329–337.

Ortega F, Pérez-Sen R, Delicado EG, Miras-Portugal MT. 2009. P2X7 nucleotide receptor is coupled to GSK-3 inhibition and neuroprotection in cerebellar granule neurons. Neurotox Res 15:193–204.

Panenka W, Jijon H, Herx LM, Armstrong JN, Feighan D, Wei T, Yong VM, Ransohoff RM, MacVicar BA. 2001. P2X7-like receptor activation in astrocytes increases chemokine monocyte chemoattractant protein-1 expression via mitogen-activated protein kinase. J Neurosci 21:7135–7142.

Pellegatti P, Raffaghello L, Bianchi G, Piccardi F, Pistoia V, Di Virgilio F. 2008. Increased level of extracellular ATP at tumor sites: In vivo imaging with plasma membrane luciferase. PLoS ONE 3:e2599.

Poulikakos PI, Solit DB. 2011. Resistance to MEK inhibitors: should we co-target upstream? Sci Signal 4:pe16.

Rangel-Yescas GE, Vazquez-Cuevas FG, Garay E, Arellano RO. 2012. Cloning and functional analysis of P2X1b, a new variant in rat optic nerve that regulates the P2X1 receptor in a use-dependent manner. Acta Neurobiol Exp (Wars) 72:18–32.

Rodrigues MA, Gomesv DA, Leite MF, Grant W, Zhang L, Lam W, Cheng YC, Bennett AM, Nathanson MH. 2007. Nucleoplasmic calcium is required for cell proliferation. J Biol Chem 282:17061–17068.

Runnebaum IB, Stickeler E. 2001. Epidemiological and molecular aspects of ovarian cancer risk. J Can Res Clin Oncol 127:73–79.

Saldaña C, Garay E, Rangel GE, Reyes LM, Arellano RO. 2009. Native ion current coupled to purinergic activation via basal and mechanically induced ATP release in *Xenopus* follicles. J Cell Physiol 218:355–365.

Sauer H, Hescheler J, Wartenberg W. 2000. Mechanical strain-induced Ca(2 +) waves are propagated via ATP release and purinergic receptor activation. Am J Physiol Cell Physiol 279:C295–C307.

Slater M, Danieletto S, Gidley-Baird A, Teh LC, Barden JA. 2004a. Early prostate cancer detected using expression of non-functional cytolytic P2X7 receptors. Histopathology 44:206–215.

Slater M, Danieletto S, Pooley M, Teh LC, Gidley-Baird A, Barden JA. 2004b. Differentiation between cancerous and normal hyperplastic lobules in breast lesions. Breast Can Res Treat 83:1–10.

Selzner N, Selzner M, Graf R, Ungethuem U, Fitz JG, Clavien PA. 2004. Water induces autocrine stimulation of tumor cell killing through ATP release and P2 receptor binding. Cell Death Differ 11:S172–S180.

Solini A, Cuccato S, Ferrari D, Santini E, Gulinelli S, Callegari MS, Dardano A, Faviana P, Madec S, Di Virgilio F, Monzani F. 2007. Increased P2X7 receptor expression and function in thyroid papillary cancer: A new potential marker of the disease? Endocrinology 149:389–396.

Stefano L, Rössler OG, Griesemer D, Hoth M, Thiel G. 2007. P2X(7) receptor stimulation upregulates Egr-1 biosynthesis involving a cytosolic Ca^{2+} rise, transactivation of the EGF receptor and phosphorylation of ERK and Elk-1. J Cell Physiol 213:36–44.

Tafani M, Schito L, Pellegrini L, Villanova L, Marfe G, Anwar T, Rosa R, Indelicato M, Fini M, Pucci B, Russo MA. 2011. Hypoxia-increased RAGE and P2X7R expression regulates tumor cell invasion through phosphorylation of Erk1/2 and Akt and nuclear translocation of NF-{kappa}B. Carcinogenesis 32:1167–1175.

Tai CJ, Kang SK, Choi KC, Tzeng CR, Leung PC. 2001. Antigonadotropic action of adenosine triphosphate in human granulosa-luteal cells: involvement of protein kinase C alpha. J Clin Endocrinol Metab 86:3237–3242.

Thompson BA, Storm MP, Hewinson J, Hogg S, Welham MJ, MacKenzie AB. 2012. A novel role for P2X7 receptor signalling in the survival of mouse embryonic stem cells. Cell Signal 24:770–778.

Vázquez-Cuevas FG, Cruz-Rico A, Garay E, García-Carrancá A, Pérez-Montiel D, Juárez B, Arellano RO. 2013. Functional expression of P2X7 receptors in ovarian surface epithelium from human and mouse. Reprod Fertil Dev 25:971–984.

Vázquez-Cuevas FG, Juárez B, Garay E, Arellano RO. 2006. ATP-induced apoptotic cell death in porcine ovarian theca cells through P2X7 receptor activation. Mol Reprod Dev 73:745–755.

Zou J, Vetreno RP, Crews FT. 2012. ATP-P2X7 receptor signaling controls basal and TNFα-stimulated glial cell proliferation. Glia 60:661–673.